

SEM ANALYSIS AS A DIAGNOSTIC TOOL FOR PHOTOVOLTAIC CELL DEGRADATION

G.O. OSAYEMWENRE*, E.L. MEYER, S. MAMPHWELI

University of Fort Hare, Institute of Technology, Private Bag X1314, Alice 5700

The importance of scanning electron microscopy (SEM) analysis as a diagnostic tool for analysing the degradation of a polycrystalline Photovoltaic cell has been studied. The main aim of this study is to characterise the surface morphology of degraded cell. In recent years, production of hetero and multi-junction solar cells has experienced tremendous growth as compared to conventional silicon (Si) solar cells. Thin film photovoltaic solar cells generally are more prone to exhibiting defects and associated degradation models. To improve the lifetime of these cells and modules, it is imperative to fully understand the cause and effect of defects and degradation models. The objective of this paper is to diagnose the observed degradation in polycrystalline silicon cells, using scanning electron microscopy (SEM). In this study poly-Si cells were characterized before and after reverse biasing. The reverse biasing was done to evaluate the cells' susceptibility to leakage currents and hotspot formation. After reverse biasing, some cells were found to exhibit hotspots as confirmed by infrared thermography. The surface morphology of these hotspot regions was then characterized using SEM. The preliminary result indicates that hotspots are formed in the regions of high inhomogeneity. Energy dispersion x-ray spectroscopy (EDX) also indicates that these regions have high levels of transitional metals and non-metals.

(Received March 16, 2015; Accepted May 4, 2015)

Keywords: Energy dispersion X-ray, affected region, Polycrystalline silicon solar cell (poly-Si), foreign element (Fn).

1. Introduction

Before Photovoltaic modules get to the end user, it's usually undergoes some standard qualification and assignment test. One of such important technical requirement tests is the hotspot endurance test. According to EN/IEC 61215 standard test, every module must pass the notable defect test [1, 2]. These test primary objectives are to determine how long the module can withstand both the internal and external factors that can cause performance failures and loss of electrical insulation or thermal breakdown. Results had shown that PV modules do fail after some time, something even before their expected life span [3]. PV modules degradation has become a huge challenge to researchers, because of the negative impact it has on PV device reliability and stability. Though there are many kinds of PV failure, but the most frequent of them is the hotspot formation, with special reference to research that have worked in this field [1-5] there is still a lot of uncertainty in this form of defect which need better and simplified understanding.

When a hot spot occurs, the low current generating cell or region in the module or cell respectively, start to act as a reverse biased to the string's current of the module or cell, causing the dissipation of energy. Therefore the region will develop a higher surface temperature when compared to the other regions [6, 7]. Though many works has been done on this topic, but little has been achieved on the physical/external effect of hot spot on PV modules/cells. The present study deals with the effect localized heat has on PV cells and the effect of degradation on PV cell. To achieve this, the structure of a degraded cell was studied. Secondly the chemical composition

*Corresponding author: gosayemwenre@ufh.ac.za

of the various region of interest across the cell was examined. Findings show that the homogeneity in the surface morphology could also be related to the chemical compositions. The development of leakage current in a module can lead to failure if preventive measures are not applied [8-10]. It has been proven that region where impurities are concentrated in semiconductor can lead to higher current leakage in the form of a shunt, this lower the quantity of current reaching the external load.

2. Experiemntal details Methods

The analytical tools employed in this study include; visual inspection, optical inspection, scanning electron microscopy (SEM) and Energy Dispersive X-Ray (EDX) [11]. For optical inspection an optical microscope was employed to scan through the surface of each of the cells and no visible defect was found. Figure 1 present one of the polycrystalline solar cell, with a manufacturer rating of: dimension (156×156)mm, power of 4W, short circuit current of 8amp and a voltage of 0.5V.



Fig. 1. 156mm by 156mm Polycrystalline solar cell

2.1 Electrical characterization

The electrical characterization of each cell was done before creating defects in the cells and the results show each has uniform performance parameters. The block diagram of the experimental set up is show in figure 2.

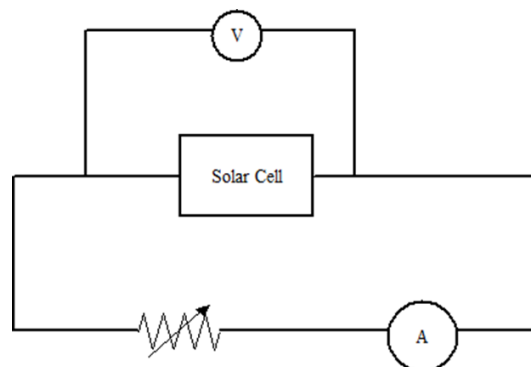


Fig. 2. Illustrating the I-V characterization of the cell using the variable resistor method

The electrical characterization was done indoor, using a simulating lamp of 1000w/m² irradiance at 25°C room temperature. Figure 2 depicts the systematic diagram used for the defect formation, where 'A' represents the ammeter; 'V' is the source of the power supplier. After the characterization an 11 volt rated Hantek programmable high precision lab bench DC power

supplier was used to supply electric power to the cell in reverse biased mode [12], this was done to test the susceptibility of the cells to linkage current [1, 12]. The poly-Si cells were later characterized after the linkage current investigation and the results reveal the degradation of two cells (performance parameter) as well as hot spot formation, the cell with worst case scenario was used for further analysis.

2.2 Scanning electron microscopy (SEM)

2.2.1 Experimental procedure background

Five polycrystalline silicon solar cells (poly-Si), which were newly supplied, were subjected to hot spot investigation with IR (infra-red) camera and they were all found to be in good condition judging from their uniform temperature distribution. Next was the introduction of defect by supplying an external voltage to the cell in the reverse mode at 11V biasing voltage, this was done for all the cells. The defect creation process took about 3600seconds, theoretically as the time duration increases a complete breakdown in some region will occur in the absence of potential difference across the pn junction [13-16].

During the reverse mode, the band gap begins to increase resulting in the reduction of the amount of electron reaching the conduction band from the valence band, until no current flow from the valence band to the conduction band when this happens a complete breakdown is said to have occurred [3, 14]. Simultaneously at the same time a hot spot investigation was carried out during the reverse mode using IR camera [17]. From the IR images some regions were discovered to have developed hotspots, in the defected cells [17-18]. From one of the defective cell three samples were prepared as follows: hot spot region (sample A), the region immediately after hot spot centre (sample B), and non-affected region (sample C).

2.2.2 Sample preparation for SEM analysis.

Sample A, B and C were cut into smaller size of 9mm× 9mm and place on the stubs using carbon double side tab, before introducing into the JEOL JSM-6390LV (SEM) device with an accelerated voltage of 12keV. This uniform acceleration voltage helps to maintain uniform sample-electron beam interaction across the sample morphology, for detail refer to [12, 17]. The SEM micrographs revealed the defected region in the cell. Each region of interest was diagnosed with EDX for chemical composition analysis.

The main purpose of EDX analysis was to identify the elemental composition of the various regions. From this work we can assume that the elemental composition at various region play a major part in PV cell defect formation, since no new constituent elements are introduced during the reverse biasing process. Though the elemental composition of the module might have change form, due to impact ionization, moisture and electrolytic process after a long exposure in the case of outdoor deployment.

3. Results and discussions

3.1. Structural analysis

Table 1; show the electrical characterization results of the cell used for analysis, it gives the performance parameters before and after the defect formation.

Table 1: Performance parameter characterization

Parameter	Measurement before reverse biasing			Measurement after reverse biasing		
	I_{sc} (mA)	V_{oc} (V)	P_{max} (W)	I_{sc} (mA)	V_{oc} (V)	P_{max} (W)
Value	7.82	0.50	3.88	2.63	0.45	1.12
% Diff	-	-	-	50.3	4.5	45.4

The performance parameters results show the effect of degradation on the PV cell. The percentage difference in the short circuit current, potential difference and maximum power are 50 %, 4.6 % and 45.4% respectively. The decreased in performance parameter is due to the degradation caused by hot spot formation in the affected region. This means, that some regions within the cell are more prone to defect when compared to other areas where there is no sign of defect. For clarity defect in this context refers to the hotspot region.

As the voltage (bias) increases, the inbuilt electric field intensity at the depletion region increase to a certain level where the charge carrier (electron-hole) pairs acquire enough energy to ionize the surrounding lattice atoms, which in turn induce other by creating charge carrier pairs, causing the pn junction to break down for excessive current to flow through hence an increase in the shunt path.

3.2 Elemental analysis/SEM images

3.2.1 SEM and Energy dispersive spectroscopy (EDX) analysis.

In figure 3 (3.1-3.4), the SEM micrographs of samples from both the affected and the non-affected regions are presented. Fig. 3.1 present samples from the grain boundary region while 3.1a) show the affected area and 3.1b) gives the non-affected area. Evident from fig. 3.1a) is the depletion of the Ag scribe line; this is due to the burnt experience in the area. The SEM micrographs in figure 3.2 represent samples outside the grain boundary of the affected region, the presence of structural damage is shown, and this reveals the device internal layer. The absence of surface crystal texture in figure 3.2 a) is attributed to abnormal heat content in the region. Furthermore, the black area in fig. 3.2a represents the internal layer crystal matrix which may be due to precipitations. The sample shown in fig. 3.3a was taken from another region where the hot spot was also observed and fig. 3.3 b is a section of the defective area along the grain boundary. While figure 3.4 samples show fine crystal grain structure without any damage, both 3.4 a) and 3.5 b) are the same sample but scanned with different SEM device, while fig 3.5a was scanned with emission field SEM but fig 3.5b was scanned with the conventional SEM device.

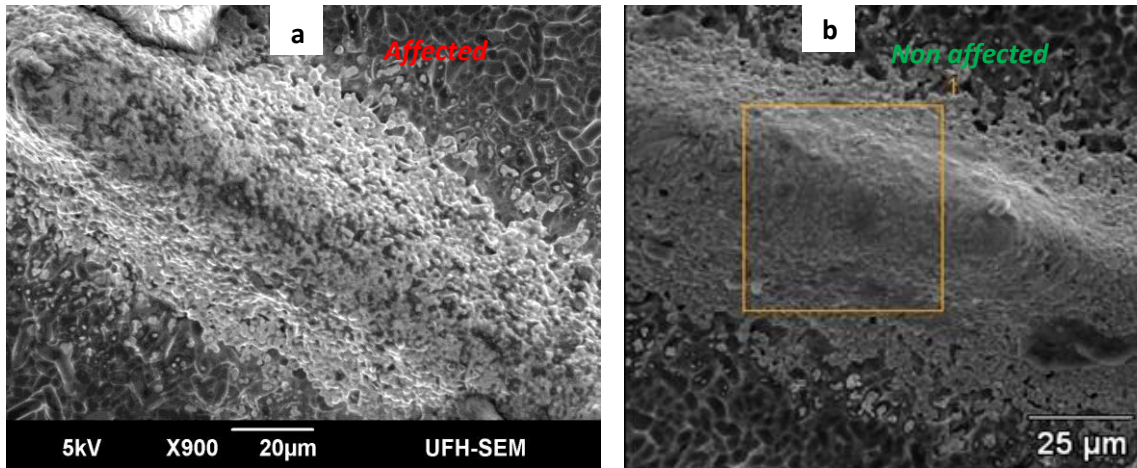


Fig. 3.1: SEM micrograph of samples from the grain boundary scanned by a conventional SEM device.

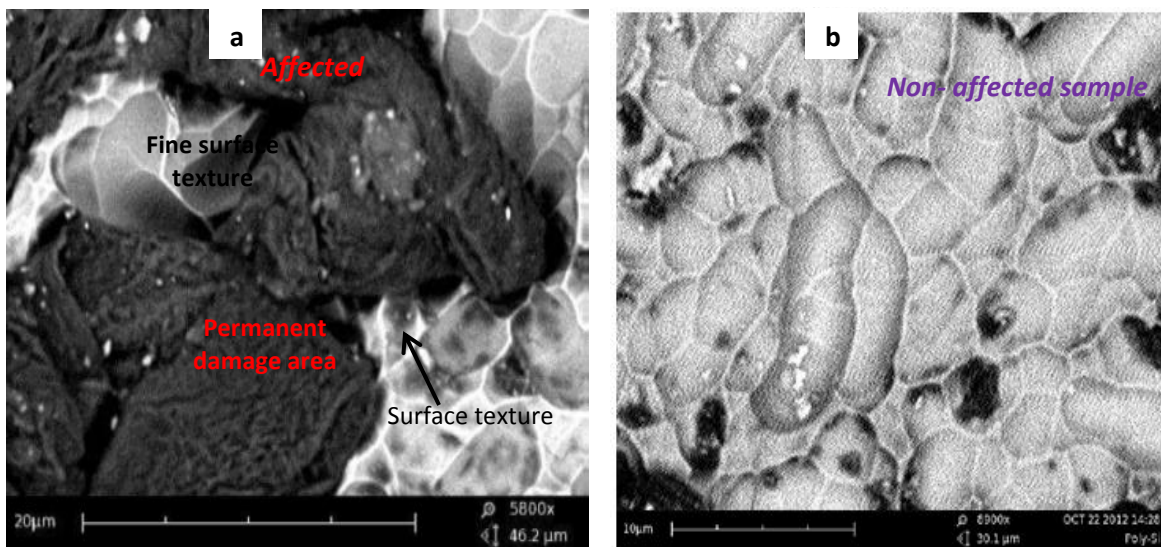


Fig. 3.2: SEM micrograph showing the (a) affected region and (b) non-affected region (scanned by emission field SEM).

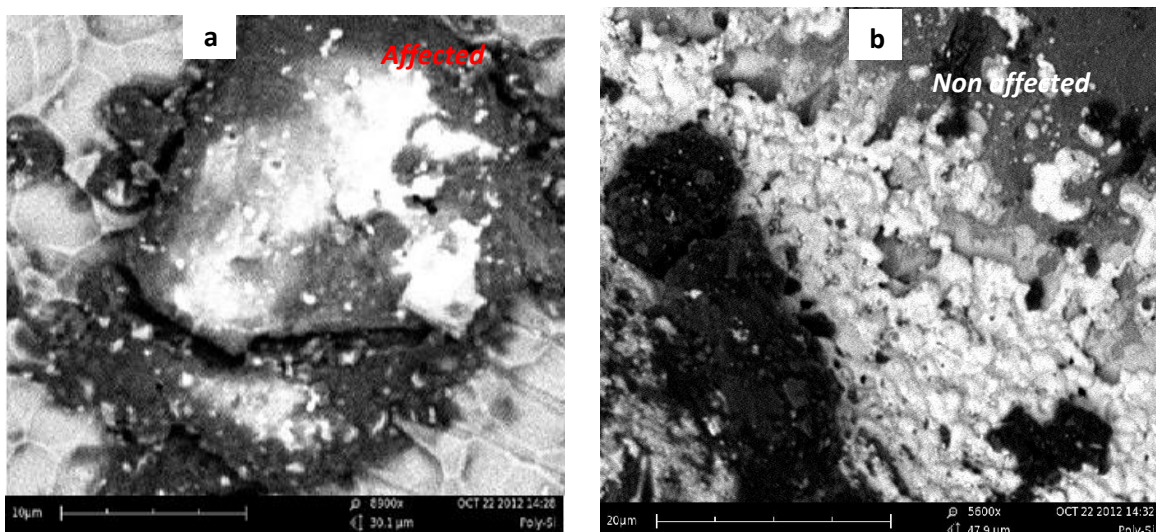


Fig. 3.3: SEM micrograph showing the (a) affected region outside the grain boundary and (b) non-affected region along the grain boundary

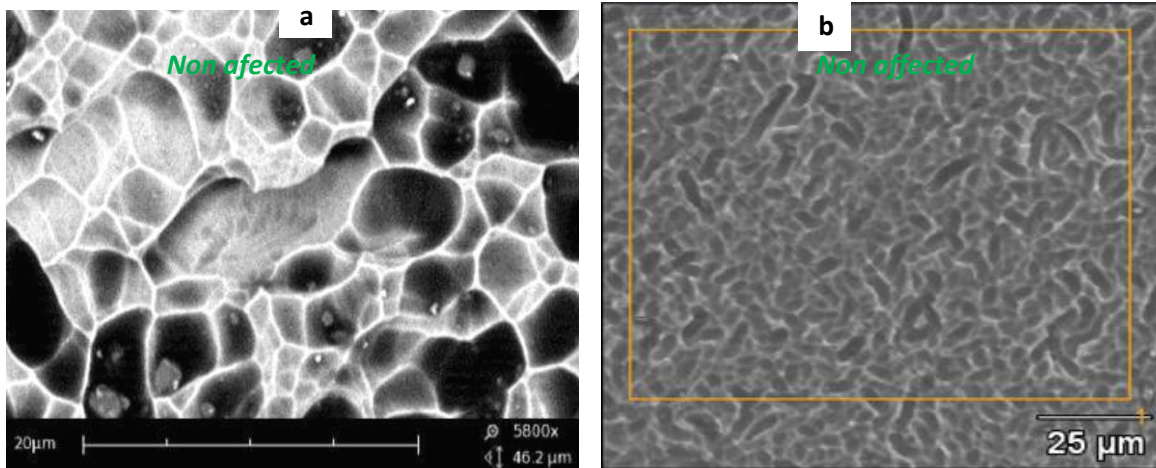


Fig. 3.4: SEM micrograph showing the (a) image of the affected region from field emission SEM and (b) non-affected region from conventional SEM.

Figure 4.1, gives the SEM image together with the EDX spectra of the sample presented in fig. 3.4b. In this micrograph the surface grain structure illustrates high degree of homogeneity. In order to characterize the chemical composition of the sample microstructure, an EDX was performed. The spectra reveal strong Si peak with little trace of sodium, why the quantity of carbon and oxygen are negligible. This spectrum represents the average elemental composition of the area marked by the orange box.

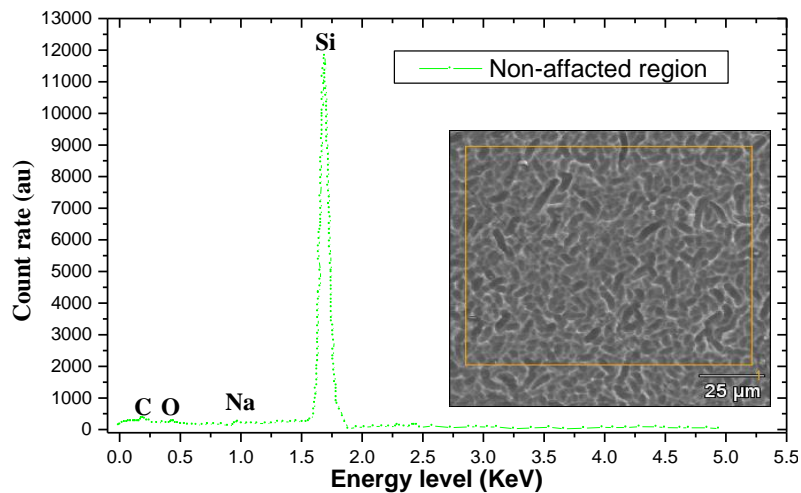


Fig. 4.1. SEM image and EDX analysis of sample in the non-affected region

The SEM image and the EDX spectra of the sample from the affected region are presented in figure 4.2. From the sample some degree of damage in the surface structure is observed, this is attributed to the irreversible destruction resulting from hot spot formation. The corresponding EDX spectra shows that high concentration of foreign element in the chemical composition. The spectra reveal strong carbon and oxygen peak, though these results are most likely to be from the antireflective coating. But the fact that there is a huge distinction between the chemical composition of elements in affected region when compared to the non-affect show that these high variations in the chemical composition may be connected to the proneness of these regions to hotspot or defect formation.

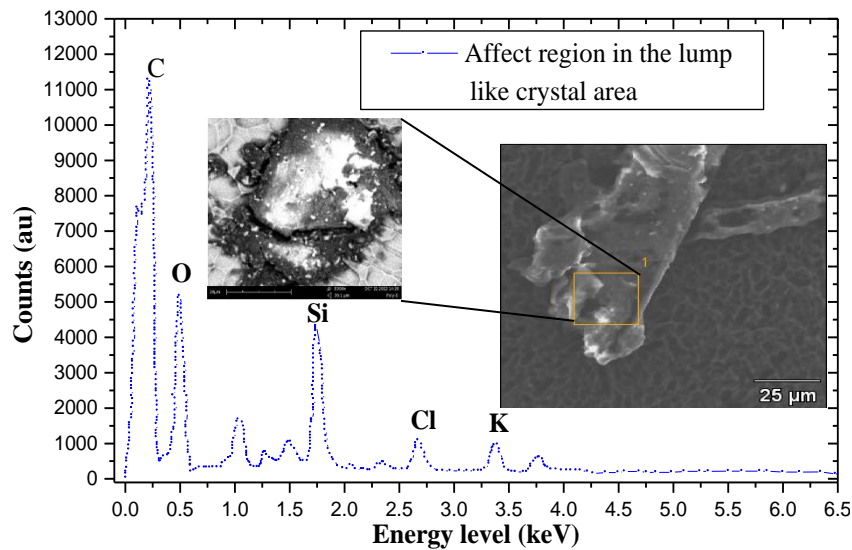


Fig. 4.2: showing the SEM image of the hot spot region and the EDX analysis (specimen X) with a temperature of $170^{\circ} C$

The major constituent element of solar cell is silicon, while the other dopants are introduced to enhance the efficiency or the stability of the device. The inconsistency in the quantity of other foreign (Fn) elements introduced can upset the Si to Fn-element ratio and when the percentage of Fn-element exceed the standard quantity it act as an impurity. From analysis, some area is found to contain more impurities than others, while the impurity kind also varies from one region to another [21-23]. From fig 4.1 to 4.3, it is clear that the hot spot region contains excessive amount of foreign element which constitute contamination. These impurities are introduced during production processes in an attempt to reduce costs by employing low grade material; the disadvantages of these impurities, is that they generate an extra energy level at the band-gap region [17-25]. Fig. 4.3, gives the EDX analysis of the sample presented in figure 3.2.

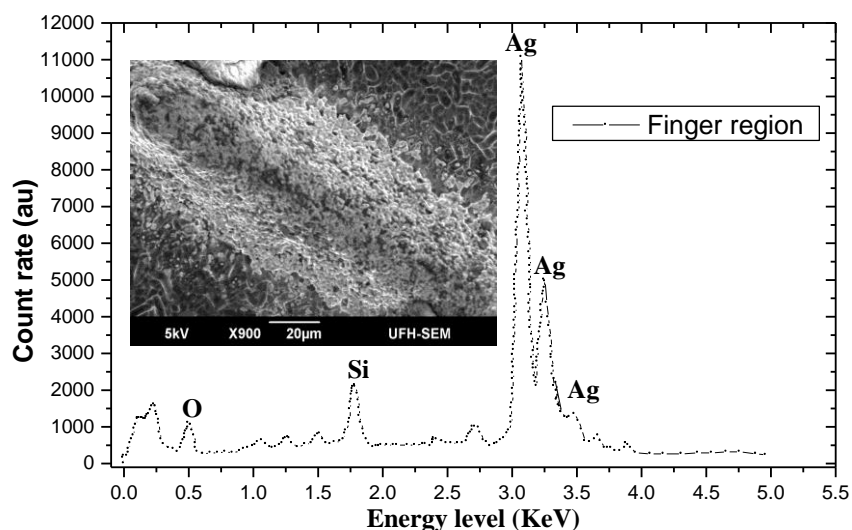


Fig. 4.3: show both the SEM image and EDX analysis of hot spot region (specimen G), at the grain boundary.

3.3 Percentage composition analysis.

Fig. 5, present the elemental composition of the analysed samples, also included is the error in the percentage weight of each element. For clarity the elemental % is the same as the weight %.

Elemental weight %			
<i>C</i>	<i>O</i>	<i>Na</i>	<i>Si</i>
4.12	1.33	0.12	94.43
Weight % Error			
<i>C</i>	<i>O</i>	<i>Na</i>	<i>Si</i>
+/-0.67	+/-0.18	+/-0.04	+/-0.37

Fig. 5.1: Percentage chemical composition of the non- affected region.

Weight %					
<i>O</i>	<i>Na</i>	<i>Al</i>	<i>Si</i>	<i>S</i>	<i>Ag</i>
4.77	0.34	0.64	2.81	0.64	90.79
Weight % Error					
<i>O</i>	<i>Na</i>	<i>Al</i>	<i>Si</i>	<i>S</i>	<i>Ag</i>
+/-0.39	+/-0.07	+/-0.05	+/-0.06	+/-0.10	+/-0.89

Fig. 5.2: Percentage chemical composition of the affected region along the grain boundary (GB).

Affected region outside GB

Weight %									
<i>C</i>	<i>O</i>	<i>Na</i>	<i>Mg</i>	<i>Al</i>	<i>Si</i>	<i>S</i>	<i>Cl</i>	<i>K</i>	<i>Ca</i>
43.92	33.36	3.64	0.64	1.12	7.97	0.56	2.95	3.76	2.08
Weight % Error									
<i>C</i>	<i>O</i>	<i>Na</i>	<i>Mg</i>	<i>Al</i>	<i>Si</i>	<i>S</i>	<i>Cl</i>	<i>K</i>	<i>Ca</i>
+/-0.76	+/-0.80	+/-0.11	+/-0.09	+/-0.15	+/-0.19	+/-0.07	+/-0.11	+/-0.13	+/-0.25

Fig. 5.3: Percentage chemical composition of sample in the affected region.

From figure 5, the elemental composition in percentage of the some of the analyzed samples was presented. These quantitative analyses show the actual quantities of chemical constituent presents in the various region of interest. For the non-affected, only 3 foreign elements are present in low concentration as shown by their peaks in figure 4.1. In figure 4.2, the Ag is the primary element with 92% why figure 4.3 shows the presence of multiple foreign elements in various concentrations with carbon and oxygen having the highest percentage concentration. Carbon has the highest concentration follow by oxygen except silicon, which is the main constituent element. This implies that hot region has a high concentration of carbon and oxygen, though the whole cell was subjected to the same degradation process.

4. Conclusion

The SEM micrographs demonstrated the destructive effect of hot spot/defects in some areas in the affected regions. While the EDX analysis, shows that the chemical composition of the elements varies with their concentration from one region to another, this buttress the fact that structural and elemental composition of the cell are inhomogeneous particularly in the affected regions. All the affected regions contain high amount of metallic contaminant, while carbon and

oxygen are present in an exceptional concentration. According to this study, there should be a safety level of impurity allowed in polycrystalline solar cell in order to maintain their reliability and stability.

Acknowledgement

This work was supported by the international affairs office University of Fort Hare and the authors gratefully acknowledged GMDRC.

References

- [1] S. Mau, T. Kramertz, J. Wolfgang, F. Hurbert, In: Proc. 19th EU PVSEC, Paris (2004).
- [2] M. A. Munoz, M. C. Alonso-Garcia, Nieves Vela, F. Chenlo, *Advance Complutense*, **22**, 28040 (2011).
- [3] E. L. Meyer, Ph.D. Thesis, submitted for the partial fulfilment of the degree of doctor of philosophy in Physics at NMMU South Africa, 74–77 (2002).
- [4] S. E. Forman, *et al.*, Proc. 14th IEEE photovoltaic specialists conference San Diego, CA, (1980) 1284.
- [5] R. Lange, PhD Dissertation at University of SIEGEN, (2000).
- [6] H. Yoshioka, *et al.*, IEEE, (1996).
- [7] W. Hermann, W. Wiesner et al., IEEE (1997).
- [8] J. Wohlgemuth, *et al.*, IEEE, (2005).
- [9] L. N. Dumas, *et al.*, IEEE, (1981).
- [10] J. W. Bishop, *Solar Cells*, **26**, 335 (1989).
- [11] N. N. Greenwood, A. Earnshaw, New York permagon press, 1185 (1984).
- [12] G. O. Osayemwenre, E. L. Meyer, *Digest J. nanomat.* **9**, 1199 (2004).
- [13] J. Wohlgemuth, W. Herrmann, *Proceedings of the 29th IEEE Photovoltaic Specialist Conference*, 889 (1994).
- [14] S. M. Sze, *Physics of Semiconductor Devices*, John Wiley and Sons, (1981).
- [15] J. Wohlgemuth, *et al.*, IEEE (1994).
- [16] C. Gonzalez, *et al.*, IEEE (2005).
- [17] T. Buonassisi, O. F. Vyvenko, A. A. Istratov, E. R. Weber, *Journal of Physics* **95**, 1556(2004).
- [18] J. F. Hamilton, *photographic science and engineering*, **18**, 493 (1974).
- [19] O. Breitenstein, *et al.*, *Progress in photovoltaic: Research and applications*, **12**, 533 (2004).
- [20] E. Molenbroek, D. W. Waddington, K.A. Emmery, IEEE, 547-552 (1991) .
- [21] C. Kittel, *introduction to solid state physics*, 8th Edition, Wiley (2005).
- [22] L. M. Slifkin, *crystal lattice defects and Amorphous materials* **18**, 81 (2007).
- [23] A. Pegels, *Renewable energy in South Africa*. *Energy* **38** (2010).
- [24] J. A. Mazer, *Solar cells: an introduction to crystalline photovoltaic Technology*, Kluwer Academic. (1997).
- [25] V. Quaschnig, *Solar Energy*, **56**, 513 (1996)